Mechanisms of Aortic and Cardiac Dysfunction in Uremic Mice With Aortic Calcification

Julien Maizel, MD*; Isabelle Six, PhD*; Michel Slama, MD; Christophe Tribouilloy, MD, PhD; Henry Sevestre, MD; Sabrina Poirot, Tech; Philippe Giummelly, PhD; Jeffrey Atkinson, PhD; Gabriel Choukroun, MD, PhD; Michel Andrejak, MD; Said Kamel, Pharm D, PhD; Jean Claude Mazière, MD, PhD; Ziad A. Massy, MD, PhD

Background—Chronic renal failure (CRF) is associated with cardiac dysfunction and increased aortic stiffness. The mechanisms involved are not clearly understood. We examined changes over time in cardiac and aortic function in a murine CRF model.

Methods and Results—Eight-week-old mice were randomly assigned to 1 of 4 groups: wild-type non-CRF, wild-type CRF, apolipoprotein E knockout non-CRF, and apolipoprotein E knockout CRF. Echocardiography was performed and blood samples were taken at baseline and after 6 and 10 weeks of CRF. Vascular reactivity and adhesion molecule expression were studied after 6 and 10 weeks of CRF. Left ventricular hypertrophy, altered left ventricular relaxation, and increased aortic stiffness were observed after 6 weeks of CRF and persisted after 10 weeks. The 4 groups of mice did not significantly differ in terms of arterial blood pressure and aortic structure. The degree of vascular calcification and serum total cholesterol concentration were higher in the CRF groups than in the non-CRF groups. These changes, however, could not explain the cardiac and vascular differences seen in the 2 CRF groups. In contrast, alterations in vascular reactivity, the upregulation of adhesion molecule expression, and CRF status were significantly associated with these changes.

Conclusions—In a mouse model of CRF, left ventricular hypertrophy, cardiac diastolic dysfunction, and increased aortic stiffness were not related to structural changes in the aorta (including aortic calcification) or high serum cholesterol levels. However, cardiac and aortic abnormalities were associated with the extent of subendothelial dysfunction and the severity of CRF. (***Circulation*. 2009;119:306-313.)**

Key Words: kidney failure, chronic ■ echocardiography ■ uremia

Cardiovascular disease is highly prevalent in patients with chronic kidney disease (CKD) and may account for 50% of all deaths.[1] Several well-known, archetypal risk factors such as age, hypertension, cigarette smoking, lipid abnormalities, and diabetes mellitus have been found to be associated, although not consistently, with the markedly higher incidence of cardiovascular disease in these patients.[2] However, these traditional risk factors for cardiovascular disease appear to only partially explain the observed increase in cardiovascular risk. More recently, the role of new, nontraditional risk factors has repeatedly been emphasized.[3,4] Of these, aortic stiffness and left ventricular (LV) hypertrophy have emerged as new potential risk factors because recent studies have established that aortic stiffness as assessed by a higher pulse-wave velocity (PWV) is an independent predictor of all-cause and cardiovascular mortality in CKD stage 5D patients.[5,6]

Clinical Perspective p 313

The limited data in the literature suggest that cardiovascular calcification (especially aortic medial calcification) is involved in the development of aortic stiffness and in the subsequent pathogenesis of isolated systolic hypertension and LV hypertrophy.[7,8] A close correlation was found between aortic stiffness (via the PWV) and the degree of coronary artery, vascular, and valvular calcification.[8,9] However, those studies were limited to a hemodialyzed end-stage renal disease population. Moreover, there are few available data on PWV in mild to moderate CKD.[10,11] Thus, the precise temporal relationship between aortic stiffness and cardiovascular calcification in mild to moderate CKD patients remains largely unknown. Major medial calcifications are certainly an important factor in aortic stiffness alteration.[12] However, the development of mild to moderate calcifications such as those observed in earlier stages of CKD may not necessarily correlate with the development of aortic PWV alterations.

To examine the incidence of aortic stiffness, LV hypertrophy, and cardiovascular calcifications, the extent of which currently remains poorly described for the earliest stages of CKD, we decided to use a well-defined animal model of

Received September 18, 2007; accepted October 23, 2008.

From INSERM, Unit ERI-12 (J.M., I.S., M.S., C.T., S.P., G.C., M.A., S.K., J.C.M., Z.A.M.), and Jules Verne University of Picardie and Amiens University Medical Center (J.M., I.S., M.S., C.T., H.S., G.C., M.A., S.K., J.C.M., Z.A.M.), Amiens, and Pharmacology Laboratory, Pharmacy Faculty, Henri Poincaré University, Nancy (P.G., J.A.), France.

*The first 2 authors contributed equally to this work.

Correspondence to Professor Ziad A. Massy, MD, PhD, INSERM ERI-12, University of Picardie and Amiens University Medical Center, Clinical Pharmacology and Nephrology Divisions, Avenue René Laennec, F-80054 Amiens, France. E-mail massy@u-picardie.fr

Circulation **is available at http://circ.ahajournals.org** **DOI: 10.1161/CIRCULATIONAHA.108.797407**

chronic renal failure (CRF) to study accelerated atherosclerosis and vascular calcification[13,14] and to analyze the time course of changes in cardiac and aortic function parameters and the potential association of the latter with aortic calcification and other CRF-related abnormalities.

Methods

Animals and Diet

All experiments were performed in female mice purchased from Charles Rivers (Lyon, France). The animals were housed in polycarbonate cages in temperature- and humidity-controlled rooms with a 12:12-hour light-dark cycle and were given standard chow (Harlan Teklad Global Diet 2016, Harlan, Oxon, UK) and tap water ad libitum. The components of the diet (as listed by the manufacturer) were 4.2% (wt/wt) fat, 16.7% protein, 60.89% carbohydrates, 0.98% calcium, 0.25% sodium, and 0.65% phosphorus. The study was performed in 2 different mouse models: apolipoprotein E gene knockout mice (ApoE$^{-/-}$) and C57 black wild-type (WT) mice. All mice were handled in accordance with French legislation, and the protocol was approved by an institutional animal care committee.

Experimental Procedures

At 8 weeks of age, 69 WT and 76 ApoE$^{-/-}$ mice were randomly assigned to 1 of the following 4 groups: 32 WT mice without CRF (WT non-CRF; group 1), 37 WT mice with CRF (WT CRF; group 2), 33 ApoE$^{-/-}$ mice without CRF (ApoE$^{-/-}$ non-CRF; group 3), and 43 ApoE$^{-/-}$ mice with CRF (ApoE$^{-/-}$ CRF; group 4). There were more mice in the CRF and ApoE$^{-/-}$ groups to compensate for the higher anticipated postoperative mortality in these groups. As previously described, a 2-step procedure was used to create CRF.[13,14] Briefly, we applied cortical electrocautery to the right kidney through a 2-cm flank incision and then performed left total nephrectomy through a similar incision 2 weeks later. Control animals underwent sham operations, including decapsulation of both kidneys. Special care was taken to avoid damage to the adrenal glands.

Serum Biochemistry and Hematocrit

Blood samples were collected after each echocardiography session (at baseline and at 6 or 10 weeks after nephrectomy or the second sham operation). Blood samples were drawn throughout a retroorbital sinus puncture as previously described[13,14] or via a cardiac puncture during euthanasia. Serum urea, total cholesterol, phosphorus, and calcium levels were measured with a Hitachi 917 autoanalyzer (Roche, Meylan, France). The hematocrit was measured with the microcapillary centrifugation method.

Echocardiography

Seventeen WT non-CRF, 21 WT CRF, 17 ApoE$^{-/-}$ non-CRF, and 28 ApoE$^{-/-}$ CRF mice were randomly assigned to a transthoracic echocardiography (TTE) procedure. Each TTE was followed by blood sampling to determine serum urea, total cholesterol, phosphorus, calcium, and hematocrit. The first TTE was performed at baseline (1 week before nephrectomy or second sham operation) in a subgroup of mice in each group as follows: 9 WT non-CRF, 11 WT CRF, 10 ApoE$^{-/-}$ non-CRF, and 15 ApoE$^{-/-}$ CRF. The second (intermediate) TTE was performed in all mice 6 weeks after nephrectomy or the second sham operation. The third and final TTE was performed after 10 weeks after nephrectomy or the second sham operation in the mice that had not been sacrificed after 6 weeks of CRF as follows: 5 WT non-CRF, 7 WT CRF, 5 ApoE$^{-/-}$ non-CRF, and 9 ApoE$^{-/-}$ CRF. Briefly, TTE examinations were performed under isoflurane inhalation general anesthesia with a heart rate of ≈400 to 450 bpm. Isoflurane was administered with a vaporizer. After induction in an isolated chamber (3.5% to 4.5% isoflurane), anesthesia was maintained with 0.5% to 0.75% isoflurane delivered through a small nose cone. TTE measurements were performed in the left lateral decubitus position with a commercially available echocardiograph (Philips Agilent 4500, Philips, Massy, France) with a 12-MHz transducer. M-mode echocardiography of the left ventricle was performed to measure the following parameters: LV end-diastolic dimension (LVDD), LV end-systolic dimension (LVSD), diastolic posterior wall thickness (PW), and diastolic septal wall thickness (SW) according to the American Society of Echocardiography guidelines.[15] LV mass (LVM) was calculated from the following formula: $LVM=1.04\times[(LVDD+PW+SW)^3-LVDD^3]$. The aortic root dimension was measured on the M-mode image obtained just above the sinotubular junction in systole (DAos) and diastole (DAo). The systolic expansion rate of the aorta (ESAo) was calculated as follows: $ESAo=(DAos-Dao)/DAo$.

The isovolumic relaxation time (IVRT) was measured, and the Tei index was calculated (difference between the duration of diastole and that of mitral flow divided by the ejection time[16]) using mitral pulsed Doppler.

Blood Pressure and PWV Measurements

Six or 10 weeks after nephrectomy or the second sham operation, mice were anesthetized with a mixture of ketamine and xylazine, and a Millar Mikro-tip 1.4F pressure transducer (outer diameter, 0.47 mm; Millar Instruments, Houston, Tex) was introduced through the aortic arch into the right carotid artery to measure intravascular arterial blood pressure. Systolic arterial, diastolic arterial, mean arterial blood, and pulse pressures were calculated by the data acquisition system (EMKA technologies, Paris, France) by averaging over at least 30 consecutive seconds. Next, the abdominal aorta or the femoral artery was exposed. A second Millar Mikro-tip pressure transducer was inserted directly into the abdominal aorta or through the femoral artery. When blood pressure and heart rate were stable, the 2 pressure waves were recorded simultaneously for at least 3 minutes. The propagation time for the pulse wave moving from the aortic arch to the abdominal aorta was measured by the time interval between the upstroke (foot) of each pressure wave front. Measurements were performed by averaging at least 10 consecutive, normal cardiac cycles. After euthanasia, the aorta was exposed, and the distance between the 2 transducers (ie, the pulse-wave propagation distance) was determined with a cotton thread. The PWV was obtained by dividing this distance by the time interval between the 2 pressure wave fronts.

After 6 weeks of CRF, 1 ApoE$^{-/-}$ CRF mouse died of bleeding during the invasive blood pressure measurement. After 10 weeks of CRF, 1 WT non-CRF, 2 ApoE$^{-/-}$ non-CRF, and 4 ApoE$^{-/-}$ CRF mice died of bleeding during invasive blood pressure measurement.

Histological Procedures

Six and 10 weeks after nephrectomy or the second sham operation, animals were killed for histological examination and immunostaining of endothelial cells and adhesion molecules. Mice were anesthetized with ketamine and xylazine (100 and 20 mg/kg), and a blood sample for serum biochemistry was collected by cardiac puncture. The heart and aorta were dissected down to the renal arteries and removed. The heart and aortic root were separated from the more distal aorta as previously described.[13,14]

Aortic calcifications were quantified in all mice assigned to the TTE procedure with Von Kossa staining and semiautomated measurement software. The precision and accuracy of this method have been reported elsewhere.[13,17] Data were expressed as the relative proportion of the calcified area to the total surface area.

In all mice assigned to a TTE procedure, the quantification of atherosclerotic lesions with an Oil Red O staining was performed with Histolab software (Microvision Instruments, Evry, France) as previously described.[13,14]

Six weeks after nephrectomy or the second sham operation, a sample of frozen aorta was removed and weighed (1 to 2 mg) for 6 WT non-CRF, 7 WT CRF, 7 ApoE$^{-/-}$ non-CRF, and 5 ApoE$^{-/-}$ CRF mice. Aortic wall collagen, elastin, and the content of the elastin-specific cross-linking amino acids desmosine and isodesmosine were determined by capillary zone electrophoresis and ultraviolet detection after hydrochloric acid hydrolysis.[18] For technical reasons, this procedure could not be performed after 10 weeks of uremia.

Six and 10 weeks after nephrectomy, 27 and 28 mice were randomly assigned for evaluation of endothelial cells and adhesion molecules, respectively, in the aortic root via the immunostaining of

Table 1. Effect of ApoE$^{-/-}$ and CRF on Baseline Body Weight, Serum Biochemistry, and Hematocrit

	WT Non-CRF (n=9)	WT CRF (n=11)	ApoE$^{-/-}$ Non-CRF (n=10)	ApoE$^{-/-}$ CRF (n=15)	Effect of ApoE/CRF/Interaction *P*
Body weight, g	18.8±1.6	17.9±0.7	18.4±1.2	18.0±1.1	NS/NS/NS
Urea, mmol/L	7.9±1.0	10.5±1.9	7.2±1.5	9.1±1.6	NS/0.002/NS
Calcium, mmol/L	2.10±0.20	2.11±0.30	2.18±0.05	2.14±0.17	NS/NS/NS
Phosphorus, mmol/L	2.47±0.34	2.46±0.19	2.54±0.35	2.19±0.35	NS/NS/NS
Cholesterol, mmol/L	1.9±0.2	2.1±0.2	6.1±2.3	8.6±1.7	0.0001/0.03/NS
Hematocrit, %	37.0±3.1	35.8±3.0	38.8±2.0	37.2±2.6	NS/NS/NS

4-μm sections of aortic tissue. Briefly, 3 nonconsecutive 4-μm-thick sections were selected at random for each artery. Sections were incubated with peroxidase blocking reagent before incubation for 60 minutes at room temperature with biotinylated monoclonal antibodies (intercellular adhesion molecule-1 [ICAM-1]: CD 54, catalog No. 553550, dilution 1:25; vascular cell adhesion molecule-1 [VCAM-1]: CD 106, catalog No. 553331, dilution 1:100; PharMingen, San Diego, Calif; CD31, catalog No. sc-1506, dilution 1:25 from Santa Cruz Biotechnology, Santa Cruz, Calif). After rinsing with PBS, sections were treated with peroxidase-labeled streptavidin for 30 minutes, followed by incubation with 2% 3,3′-diaminobenzidine in substrate buffer. Mayer's hematoxylin was used as a counterstain. Sections were dehydrated with a series of alcohol dilutions and coverslipped in Pertex mounting media.

Cross sections were studied to quantify CD31, ICAM-1, and VCAM-1 immunostaining at the luminal surface. In each section, the respective percentage coverage with CD31, VCAM-1, and ICAM-1 was measured with Histolab software (Microvision Instruments, Evry, France). Endothelium integrity was defined as 100% immunostaining with CD31.

Vascular Reactivity Analysis

Six weeks after nephrectomy or the second sham operation, 32 mice were assigned for vascular reactivity analysis as follows: 8 WT non-CRF, 9 WT CRF, 8 ApoE$^{-/-}$ non-CRF, and 7 ApoE$^{-/-}$ CRF animals. Ten weeks after nephrectomy or the second sham operation, 29 mice were assigned for vascular reactivity analysis as follows: 7 WT non-CRF, 7 WT CRF, 7 ApoE$^{-/-}$ non-CRF, and 8 ApoE$^{-/-}$ CRF animals.

The descending thoracic aortas were excised rapidly and placed in oxygenated Krebs-Henseleit solution. The vascular rings were prepared as described previously[19] in adapting the technical to the mouse aorta. The vascular rings were stretched to 1.3 g (previously determined as the optimal point of their length-tension relationship). All rings were preconstricted with KCl (70 mmol/L) and, after washout, phenylephrine (from 10^{-9} to 3×10^{-5} mol/L). Endothelium function was measured as the relaxation response to acetylcholine (from 10^{-9} to 3×10^{-5} mol/L).

Statistical Analysis

Serum biochemistry, hematocrit, body weight, histological (CD31, ICAM-1, and VCAM-1, expression) data, and hemodynamic parameters were examined in a 2-way ANOVA that took into account the status of the animal (presence or absence of ApoE$^{-/-}$, presence or absence of CRF, and the interaction between ApoE$^{-/-}$ and CRF). Echocardiographic data were analyzed with a mixed-effect model considering random effects for each mouse and fixed effects for groups and time. A Wilcoxon test was used to compare the echocardiographic parameters between baseline and 6 or 10 weeks for each group separately. Relaxation responses were expressed as the percentage reduction in maximum vascular phenylephrine-induced tension. Mean intergroup differences were tested with repeated-measures ANOVA. If a significant value was found, Scheffé's test for multiple comparisons was applied. Relationships between biochemistry data, histological findings, echocardiographic findings, and PWV were analyzed by simple or multiple regression analysis. Results were expressed as mean±SD except for vascular reactivity and endothelial marker data, which are expressed as mean±SEM. Intergroup differences were considered significant at values of $P<0.05$.

The authors had full access to and take full responsibility for the integrity of the data. All authors have read and agree to the manuscript as written.

Results

Serum Biochemistry, Hematocrit, Body Weight, and Echocardiography Findings

Data on body weight, serum biochemistry, and hematocrit at baseline and after 6 and 10 weeks of CRF are shown in Tables 1 through 3. Hematocrit was measured in all the mice in the ApoE$^{-/-}$ non-CRF group except 1 (for technical reasons). Serum urea levels observed at 10 weeks were slightly but not significantly lower than those observed at 6 weeks.

Echocardiographic findings are presented in Figure 1. After 6 weeks of CRF, LV mass, IVRT, and the Tei index had significantly increased in both the ApoE$^{-/-}$ and WT CRF groups compared with the non-CRF groups. ESAo was significantly lower in the CRF groups than in non-CRF groups. These abnormalities persisted after 10 weeks of CRF. A progressive increase in LV mass over time was observed in all groups of mice, but this increase was significantly greater in groups with CRF (Figure 1).

Table 2. Effect of ApoE$^{-/-}$ and CRF on Body Weight, Serum Biochemistry, and Hematocrit After 6 Weeks of CRF

	Wild-Type Non-CRF (n=17)	Wild-Type CRF (n=21)	ApoE$^{-/-}$ Non-CRF (n=18)	ApoE$^{-/-}$ CRF (n=28)	Effect of ApoE/CRF/Interaction *P*
Body weight, g	20.4±1.6	19.2±1.5	20.3±1.2	18.9±1.3	NS/0.001/NS
Urea, mmol/L	9.6±1.77	32.5±12.5	7.72±1.3	36.7±16.3	NS/0.001/NS
Calcium, mmol/L	2.3±0.09	2.56±0.13	2.18±0.26	2.47±0.27	0.04/0.001/NS
Phosphorus, mmol/L	2.47±0.3	2.47±0.38	2.29±0.46	2.31±0.42	NS/NS/NS
Cholesterol, mmol/L	1.8±0.2	2.4±0.4	6.4±2.1	13.7±2.8	0.001/0.001/0.001
Hematocrit, %	37.5±3	27.8±3.4	35.9±3.5	28±3.7	NS/0.001/NS

Table 3. Effect of ApoE$^{-/-}$ and CRF on Body Weight, Serum Biochemistry, and Hematocrit After 10 weeks of CRF

	Wild-Type Non-CRF (n=5)	Wild-Type CRF (n=7)	ApoE$^{-/-}$ Non-CRF (n=5)	ApoE$^{-/-}$ CRF (n=9)	Effect of ApoE/CRF/Interaction *P*
Body weight, g	23.3±1.4	21.3±1.2	22.2±1.5	20.4±1.2	NS/0.002/NS
Urea, mmol/L	9.8±1.7	22.7±3.8	9.2±0.8	28±4.3	NS/0.001/NS
Calcium, mmol/L	2.22±0.09	2.54±0.1	2.12±0.2	2.43±0.2	NS/0.008/NS
Phosphorus, mmol/L	2.58±0.7	2.92±0.3	2.84±0.6	2.45±0.6	NS/NS/NS
Cholesterol, mmol/L	1.6±0.6	2.2±0.1	4.7±1.1	11.4±2.3	0.001/0.005/0.002
Hematocrit, %	34.6±3.1	31.9±3.4	33.6±2.1	29.8±2.9	NS/0.01/NS

No significant relationships between ESAo on one hand and hematocrit or serum urea on the other were observed in either CRF or non-CRF mice. IVRT was correlated with hematocrit (r^2=0.40, P=0.001) and ESAo (r^2=0.53, P=0.001). In terms of the other biochemical variables, only serum calcium levels after 10 weeks of CRF were negatively correlated with ESAo (r^2=0.37, P=0.002) and positively correlated with IVRT (r^2=0.42, P=0.001) and LV mass (r^2=0.32, P=0.006). Importantly, the 2 CRF mouse groups (WT and ApoE$^{-/-}$) presented similar cardiovascular abnormalities despite the intergroup difference in serum total cholesterol levels.

Arterial Blood Pressure and PWV

Systolic arterial pressure, diastolic arterial pressure, and mean arterial blood pressure (but not pulse pressure) were significantly increased after 6 and 10 weeks of follow-up in the WT non-CRF group (Table 4). In contrast, pulse pressure increased over time in both ApoE$^{-/-}$ non-CRF and ApoE$^{-/-}$ CRF mice. At 6 weeks of CRF, PWV significantly increased in CRF groups compared with non-CRF groups (Table 4). After 10 weeks of CRF, PWV remained high in the CRF groups, with no difference between the ApoE$^{-/-}$ groups and WT groups. PWV decreased significantly between 6 and 10 weeks of uremia in ApoE$^{-/-}$ CRF mice, which may be related to kidney function differences between the 2 groups. Significant relationships between PWV and hematocrit and between PWV and serum urea were observed (Figure 2). However, in a multiple regression analysis, only serum urea was significantly correlated with PWV as independent variable.

Vascular Reactivity

Vasoconstriction with phenylephrine (expressed as a percentage of KCl contraction) was similar for the various groups (data not shown). After 6 weeks of CRF, acetylcholine-induced relaxation was markedly lower in vessels from CRF animals than in vessels from non-CRF animals (Figure 3). After 10 weeks of CRF, acetylcholine-induced relaxation was markedly lower in vessels from WT animals than in vessels from ApoE$^{-/-}$ animals (Figure 3); however, the effects of CRF were attenuated by the fact that the ApoE$^{-/-}$ non-CRF mice had also developed endothelial dysfunction.

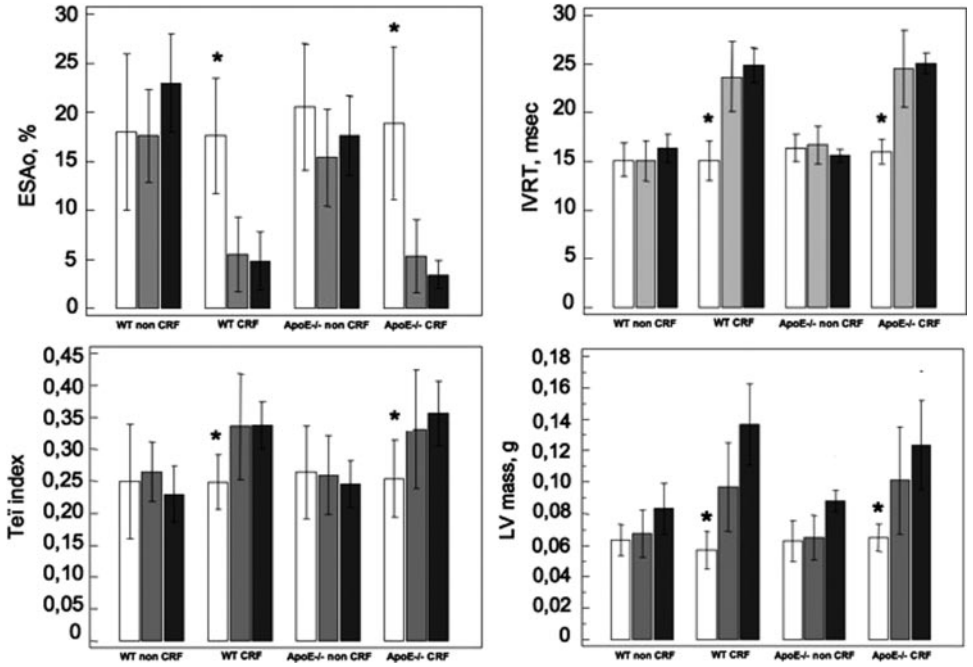

Figure 1. Changes in LV mass, IVRT, Tei index, and ESAo in each group during the experiment. Using a mixed-effect model in a global evaluation of effects for groups and time gave values of P=0.01 for ESAo, IVRT, LV mass, and the Tei index for group effects; P=0.01 for ESAo, IVRT, and LV mass; and P=0.02 for the Tei index for the change over time (baseline and 6 and 10 weeks). *P<0.05 between baseline and 6 or 10 weeks for each individual group.

Table 4. Effect of ApoE$^{-/-}$ and CRF on Invasive Hemodynamic Parameters After 6 and 10 Weeks of CRF

	WT Non-CRF	WT CRF	ApoE$^{-/-}$ Non-CRF	ApoE$^{-/-}$ CRF	Effect of ApoE/CRF/Interaction *P*
After 6 wk of CRF (4–5 mice per group)					
SAP, mm Hg	77±14	85±13	80±8	72±20	NS/NS/NS
DAP, mm Hg	49±11	50±11	54±6	45±17	NS/NS/NS
MAP, mm Hg	58±12	62±11	62±6	54±18	NS/NS/NS
PP, mm Hg	28±7	35±3	26±2	27±8	0.001/NS/NS
PWV, m/s	2.7±0.8	2.9±0.6	3.1±0.4	5±0.9	0.007/0.01/NS
After 10 wk of CRF (7–9 mice per group)					
SAP, mm Hg	94±18*	78±6	85±10	84±16	NS/NS/NS
DAP, mm Hg	59±11*	50±8	56±10	50±16	NS/NS/NS
MAP, mm Hg	71±12*	60±7	65±10	61±16	NS/NS/NS
PP, mm Hg	34±11	28±8	29±4*	34±3*	NS/NS/NS
PWV, m/s	2.5±0.4*	4.4±0.8	2.9±0.5	3.3±0.4*	NS/0.001/NS

SAP indicates systolic arterial pressure; DAP, diastolic arterial pressure; MAP, mean arterial pressure; and PP, pulse pressure.
*$P<0.05$ vs 6 weeks of CRF.

Aortic Calcifications and Atherosclerotic Lesions

CRF status and ApoE$^{-/-}$ knockout both increased aortic intimal and medial calcification after 6 and 10 weeks of follow-up (Table 5). There was no apparent relationship between the degree of calcification on one hand and the ESAo, diastolic function, or LV mass results on the other. No correlation between intimal or medial calcifications and PWV was observed. It is noteworthy that although the 2 CRF mouse groups (WT and ApoE$^{-/-}$) had similar cardiovascular abnormalities, they differed with respect to degree of vascular calcification.

Aortic Collagen, Elastin, and Desmosine Content

There were no observed differences between the 4 groups in terms of the aortic desmosine, isodesmosine, collagen, or elastin content after 6 weeks of follow-up (Table 5).

Endothelial and Adhesion Molecule Immunostaining

Endothelium immunostaining with the CD31 antibody confirmed the integrity of the endothelium in both the non-CRF and CRF groups (Figure 4). Vascular lesions of WT CRF and ApoE$^{-/-}$ CRF mice were preceded by upregulation of ICAM-1 and VCAM-1 expression in the endothelium at 6 weeks (Figure 5). In ApoE$^{-/-}$ non-CRF mice, endothelium upregulation of ICAM-1 and VCAM-1 expressions was delayed until 10 weeks (Figure 5).

Discussion

In the present study, we found that compared with non-CRF littermates, mice with a moderate degree of CRF rapidly developed a significant increase in aortic stiffness, together with LV hypertrophy and altered LV relaxation and endothelium-dependent vessel relaxation. At this stage in CRF, the observed change in aortic stiffness did not appear to be a consequence of cardiovascular calcification, morphological endothelium changes, changes in aortic collagen and elastin content, or hypercholesterolemia resulting from ApoE deletion or CRF. In contrast, modulation of adhesion molecules and potential CRF-induced cardiovascular remodeling might account for the observed changes.

Vascular stiffness, a hallmark of CKD, seems to rise in parallel with the decline in renal function.[11,20] To the best of

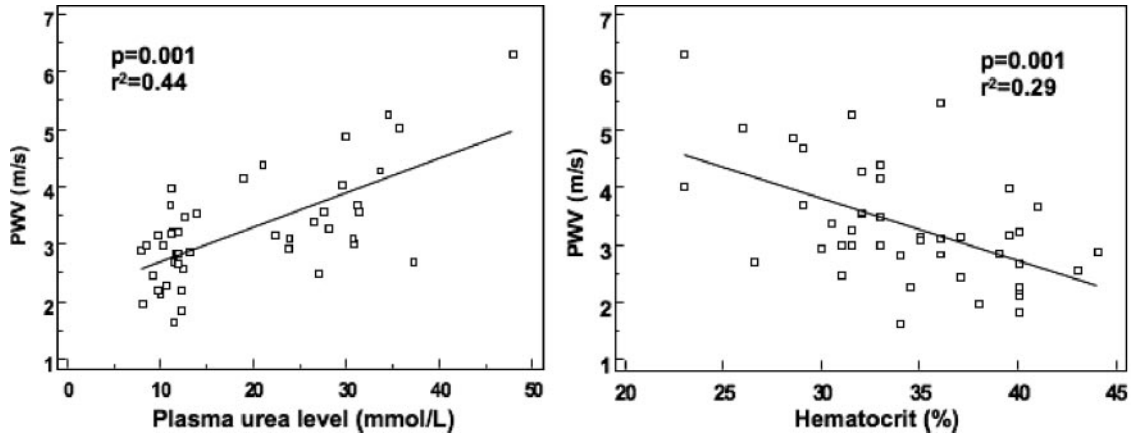

Figure 2. Relationships between the PWV and hematocrit or serum urea levels.

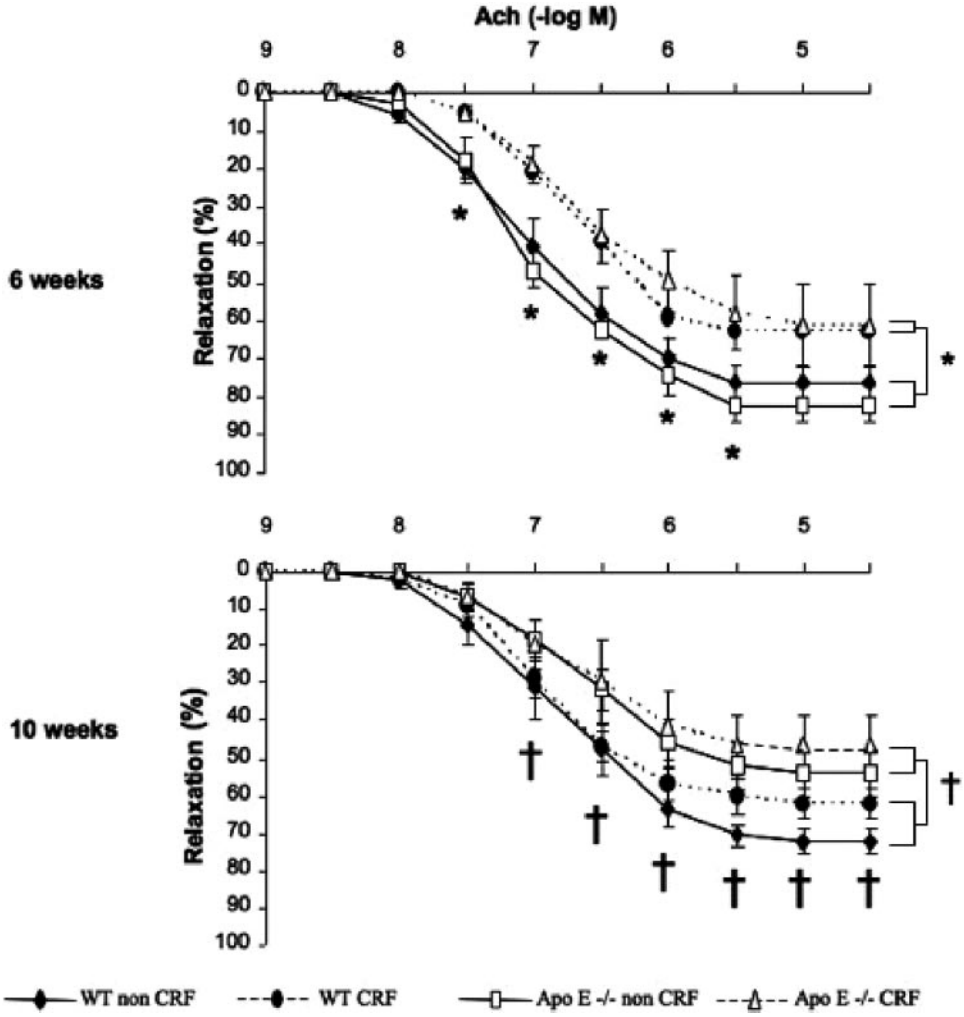

Figure 3. Vascular reactivity in each group at 6 and 10 weeks (7 to 9 mice per group). Ach indicates acetylcholine. *$P<0.05$ for non-CRF vs CRF; †$P<0.05$ for WT vs ApoE$^{-/-}$.

our knowledge, however, no longitudinal study has yet evaluated changes in vascular stiffness over the course of CKD progression. In the present study, we show for the first time that CRF mice rapidly develop a significant increase in aortic stiffness compared with non-CRF mice, as demonstrated by the observed decrease in ESAo, and increased PWV (both validated markers of aortic stiffness in mice). Interestingly, we found that 6 weeks of CRF resulted in the same degree of aortic stiffness as observed in 55-week-old non-CRF ApoE$^{-/-}$ mice (as reported by Onozuka et al[21]) and 52-week-old non-CRF ApoE$^{-/-}$ mice (as reported by Wang et al[20]). Our observation supports the hypothesis that CRF accelerates the normal, age-related changes in aortic function.

As noted above, the scarce data in the literature suggest that cardiovascular calcification (especially medial calcification) is involved in the development of aortic stiffness.[7,8] We were unable to confirm this association in our mouse model. Aortic stiffness values in the WT-CRF group were similar to those in the ApoE$^{-/-}$ CRF group, despite a significant difference in the degree of vascular calcification (see Table 5). Moreover, in the CRF groups, we did not find any relationship between aortic calcification on one hand and ESAo and PWV on the other. Our results suggest that calcification does not play a major role in the pathogenesis of vascular stiffness in the early stages of CRF. However, we cannot exclude a possible contribution of severe calcification to vascular stiffness at more advanced stages (such as stage 4 or 5 CKD[22]) because severe calcification induced by vitamin D_3 plus nicotine or by warfarin plus vitamin K_1 in rat models has been shown to be associated with increased aortic stiffness.[12,23,24] It should be noted that in these 2 animal models, the authors observed an elevation in the ratio of aortic collagen to elastin in association with the vascular calcifications, which may be the result of severe elastocalcinosis inducing destruction of elastic fibers and thus leading to arterial stiffness.[24,25] We did not observe this type of change in the ratio of aortic collagen to elastin; this could explain the absence of a correlation between vascular calcification and vascular stiffness in our present experiments.

Our results further suggest that the observed aortic hemodynamic changes are related to functional (rather than structural) changes in the aorta at this stage of CRF. The endothelial dysfunction observed in the present study is an indicator of subtle disturbances of endothelial function and could play an important role at this disease stage. The present study confirmed the results obtained by Bro et al[26] that atherosclerosis in ApoE$^{-/-}$

Table 5. Proportion of Calcified Intimal and Medial Area (Expressed as a Percentage of the Total Surface Area of Transvalvular Slices) and the Cross-Sectional Area of Atherosclerotic Lesions in the Thoracic Aorta (Expressed as a Percentage of the Total Surface Area) After 6 and 10 Weeks of Follow-Up and Collagen, Elastin, Desmosine, and Isodesmosine Aortic Contents After 6 Weeks of Follow-Up

	WT Non-CRF	WT CRF	ApoE$^{-/-}$ Non-CRF	ApoE$^{-/-}$ CRF	Effect of ApoE/CRF/Interaction *P*
6 wk of CRF					
Intimal calcification area (12–16 mice per group), %	1±1	3±2	12±2	18±9	0.001/0.02/NS
Medial calcification area (12–16 mice per group), %	1±1	2±1	4±3	6±3	0.001/0.01/NS
Atherosclerosis area (12–16 mice per group), %	0.1±0.02	0.3±0.4	12±5	11±5	0.002/NS/NS
Collagen (5–7 mice per group), μg/mg ww	60±7	55±7	50±7	54±5	NS/NS/NS
Elastin (5–7 mice per group), μg/mg ww	63±17	54±16	69±11	71±20	NS/NS/NS
Desmosine (5–7 mice per group), μg/mg ww	0.21±0.06	0.17±0.06	0.21±0.04	0.22±0.08	NS/NS/NS
Isodesmosine (5–7 mice per group), μg/mg ww	0.11±0.03	0.09±0.02	0.13±0.02	0.14±0.06	NS/NS/NS
10 wk of CRF					
Intimal calcification (5–7 mice per group), %	3±1	4±2	11±1	16±5	0.001/0.03/NS
Medial calcification (5–7 mice per group), %	1±1	2±1	3±2	6±3	0.003/0.02/NS
Atherosclerosis (5–7 mice per group), %	0±0	1±1	18±5	16±3	0.01/NS/NS

ww indicates wet weight.

CRF mice is preceded by upregulation of adhesion molecule expression in the arterial endothelium.

The present study has several limitations. First, we cannot exclude possible effects of anesthetic drugs on hemodynamic parameters. In the present study, however, echocardiography was performed in spontaneously breathing mice using inhalation anesthesia (isoflurane). Compared with other anesthetic methods, this mode of anesthesia is considered to be the least compromising with respect to hemodynamic status.[27,28] Moreover, anesthesia was necessary to slow down and equalize the high heart rate difference between groups to obtain technically comparable echocardiographic parameters. Second, we did not assess oxidative stress markers or serum levels of uremic toxins; thus, their possible contribution to LV hypertrophy and aortic stiffness cannot be excluded. We have previously shown that CRF-induced oxidative stress was associated with cardiovascular lesions and that a reduction in oxidative stress led to an improvement.[3,14]

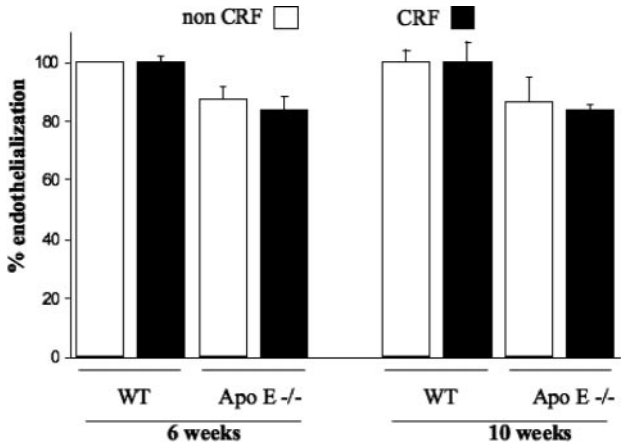

Figure 4. Quantification of endothelialization as evaluated by endothelium immunostaining with CD31 antibody in each group at 6 and 10 weeks (6 to 8 mice per group). WT non-CRF at 6 weeks was considered the control group.

Conclusions

We found that CRF mice rapidly developed LV hypertrophy, diastolic dysfunction, and aortic stiffness compared with non-CRF mice. These changes were not related to vascular calcification, high serum cholesterol levels, or structural changes in the aorta. In contrast, the degree of subtle

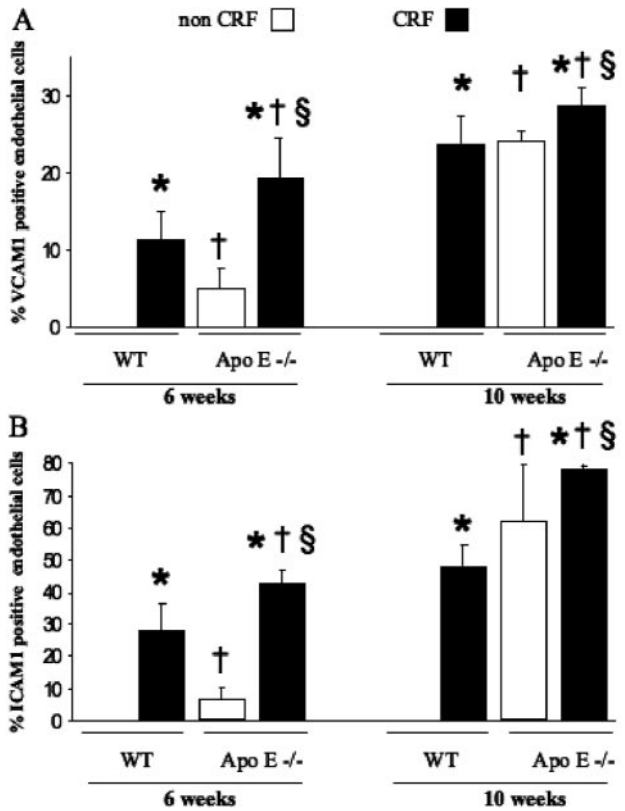

Figure 5. Quantification of adhesion molecule immunostaining in each group at 6 and 10 weeks (6 to 8 mice per group). A, VCAM-1; B, ICAM-1. *$P<0.005$ for non-CRF vs CRF; †$P<0.005$ for WT vs Apo E$^{-/-}$; §$P<0.005$ for interaction.

endothelial dysfunction and CRF status were found to be associated with the observed cardiac and aortic abnormalities.

Source of Funding

We are very grateful to the Picardie Regional Council for its unrestricted and valuable support.

Disclosures

None.

References

1. Vanholder R, Massy Z, Argiles A, Spasovski G, Verbeke F, Lameire N. Chronic kidney disease as cause of cardiovascular morbidity and mortality. *Nephrol Dial Transplant*. 2005;20:1048–1056.
2. Jungers P, Nguyen Khoa T, Joly D, Choukroun G, Witko-Sarsat V, Massy ZA. Atherosclerotic complications in chronic renal failure: epidemiology and predictive factors. *Adv Nephrol Necker Hosp*. 2000;30:177–199.
3. Ivanovski O, Szumilak D, Nguyen-Khoa T, Ruellan N, Phan O, Lacour B, Descamps-Latscha B, Drueke TB, Massy ZA. The antioxidant N-acetylcysteine prevents accelerated atherosclerosis in uremic apolipoprotein E knockout mice. *Kidney Int*. 2005;67:2288–2294.
4. Stenvinkel P, Carrero JJ, Axelsson J, Lindholm B, Heimbürger O, Massy Z. Emerging biomarkers for evaluating cardiovascular risk in the chronic kidney disease patient: how do new pieces fit into the uremic puzzle? *Clin J Am Soc Nephrol*. 2008;3:505–521.
5. London GM, Blacher J, Pannier B, Guerin AP, Marchais SJ, Safar ME. Arterial wave reflections and survival in end-stage renal failure. *Hypertension*. 2001;38:434–438.
6. Blacher J, Guerin AP, Pannier B, Marchais SJ, Safar ME, London GM. Impact of aortic stiffness on survival in end-stage renal disease. *Circulation*. 1999;99:2434–2439.
7. Blacher J, Demuth K, Guerin AP, Safar ME, Moatti N, London GM. Influence of biochemical alterations on arterial stiffness in patients with end-stage renal disease. *Arterioscler Thromb Vasc Biol*. 1998;18:535–541.
8. Raggi P, Bellasi A, Ferramosca E, Islam T, Muntner P, Block GA. Association of pulse wave velocity with vascular and valvular calcification in hemodialysis patients. *Kidney Int*. 2007;71:802–807.
9. Haydar AA, Covic A, Colhoun H, Rubens M, Goldsmith DJ. Coronary artery calcification and aortic pulse wave velocity in chronic kidney disease patients. *Kidney Int*. 2004;65:1790–1794.
10. Mourad JJ, Pannier B, Blacher J, Rudnichi A, Benetos A, London GM, Safar ME. Creatinine clearance, pulse wave velocity, carotid compliance and essential hypertension. *Kidney Int*. 2001;59:1834–1841.
11. Briet M, Bozec E, Laurent S, Fassot C, London GM, Jacquot C, Froissart M, Houillier P, Boutouyrie P. Arterial stiffness and enlargement in mild-to-moderate chronic kidney disease. *Kidney Int*. 2006;69:350–357.
12. Bouvet C, Moreau S, Blanchette J, de Blois D, Moreau P. Sequential activation of matrix metalloproteinase 9 and transforming growth factor beta in arterial elastocalcinosis. *Arterioscler Thromb Vasc Biol*. 2008;28:856–862.
13. Massy ZA, Ivanovski O, Nguyen-Khoa T, Angulo J, Szumilak D, Mothu N, Phan O, Daudon M, Lacour B, Drueke TB, Muntzel MS. Uremia accelerates both atherosclerosis and arterial calcification in apolipoprotein E knockout mice. *J Am Soc Nephrol*. 2005;16:109–116.
14. Phan O, Ivanovski O, Nguyen-Khoa T, Mothu N, Angulo J, Westenfeld R, Ketteler M, Meert N, Maizel J, Nikolov IG, Vanholder R, Lacour B, Drueke TB, Massy ZA. Sevelamer prevents uremia-enhanced atherosclerosis progression in apolipoprotein E-deficient mice. *Circulation*. 2005;112:2875–2882.
15. Sahn DJ, DeMaria A, Kisslo J, Weyman A. Recommendations regarding quantitation in M-mode echocardiography: results of a survey of echocardiographic measurements. *Circulation*. 1978;58:1072–1083.
16. Tei C, Nishimura RA, Seward JB, Tajik AJ. Noninvasive Doppler-derived myocardial performance index: correlation with simultaneous measurements of cardiac catheterization measurements. *J Am Soc Echocardiogr*. 1997;10:169–178.
17. Angulo J, Nguyen-Khoa T, Massy ZA, Drueke TB, Serra J. Morphological quantification of aortic calcification from low magnification images. *Image Anal Stereol*. 2003;22:81–89.
18. Giummelly P, Botton B, Friot R, Prima-Putra D, Atkinson J. Measurement of desmosine and isodesmosine by capillary zone electrophoresis. *J Chromatogr A*. 1995;710:357–360.
19. Six I, Mouquet F, Corseaux D, Bordet R, Letourneau T, Vallet B, Dosquet CC, Dupuis B, Jude B, Bertrand ME, Bauters C, Van Belle E. Protective effects of basic fibroblast growth factor in early atherosclerosis. *Growth Factors*. 2004;22:157–167.
20. Wang MC, Tsai WC, Chen JY, Huang JJ. Stepwise increase in arterial stiffness corresponding with the stages of chronic kidney disease. *Am J Kidney Dis*. 2005;45:494–501.
21. Onozuka H, Fujii S, Mikami T, Yamada S, Ishimori N, Shimizu T, Furumoto T, Nakal Y, Komuro K, Nishihara K, Okamoto H, Kitabatake A. In vivo echocardiographic detection of cardiovascular lesions in apolipoprotein E-knockout mice using a novel high-frequency high-speed echocardiography technique. *Circ J*. 2002;66:272–276.
22. Sigrist M, Bungay P, Taal MW, McIntyre CW. Vascular calcification and cardiovascular function in chronic kidney disease. *Nephrol Dial Transplant*. 2006;21:707–714.
23. Marque V, Van Essen H, Struijker-Boudier HA, Atkinson J, Lartaud-Idjouadiene I. Determination of aortic elastic modulus by pulse wave velocity and wall tracking in a rat model of aortic stiffness. *J Vasc Res*. 2001;38:546–550.
24. Essalihi R, Dao HH, Yamaguchi N, Moreau P. A new model of isolated systolic hypertension induced by chronic warfarin and vitamin K1 treatment. *Am J Hypertens*. 2003;16:103–110.
25. Niederhoffer N, Lartaud-Idjouadiene I, Giummelly P, Duvivier C, Peslin R, Atkinson J. Calcification of medial elastic fibers and aortic elasticity. *Hypertension*. 1997;29:999–1006.
26. Bro S, Moeller F, Andersen CB, Olgaard K, Nielsen LB. Increased expression of adhesion molecules in uremic atherosclerosis in apolipoprotein E-deficient mice. *J Am Soc Nephrol*. 2004;15:1495–1503.
27. Collins KA, Korcarz CE, Lang RM. Use of echocardiography for the phenotypic assessment of genetically altered mice. *Physiol Genomics*. 2003;13:227–239.
28. Roth DM, Swaney JS, Dalton ND, Gilpin EA, Ross JJ. Impact of anesthesia on cardiac function during echocardiography in mice. *Am J Physiol Heart Circ Physiol*. 2002;282:H2134–H2140.

CLINICAL PERSPECTIVE

Chronic renal failure (CRF) is associated with cardiac dysfunction and increased aortic stiffness. However, the precise temporal relationship between these abnormalities in mild to moderate CRF patients remains largely unknown. To examine the changes over time in cardiac and aortic function, we decided to use a well-defined animal model of CRF. We found that compared with non-CRF littermates, mice with a moderate degree of CRF rapidly developed a significant increase in aortic stiffness, together with left ventricular hypertrophy, altered left ventricular relaxation, and endothelium-dependent vessel relaxation. At this stage in CRF, the observed change in aortic stiffness did not appear to be a consequence of cardiovascular calcification, morphological endothelium changes, changes in aortic collagen and elastin content, or hypercholesterolemia resulting from apolipoprotein E deletion or CRF. In contrast, alterations in vascular reactivity, the modulation of adhesion molecules, and potential uremic toxin-induced cardiovascular remodeling might account for the observed changes. Our results reveal that the cardiovascular lesions observed in the early stages of CRF are probably functional, which may provide an opportunity to heal this damage by the use of adequate therapeutic strategies. If the present findings obtained in mice can be extrapolated to the condition in humans, this paradigm will be of major importance for patients with mild to moderate CRF.

Mechanisms of Aortic and Cardiac Dysfunction in Uremic Mice With Aortic Calcification

Julien Maizel, Isabelle Six, Michel Slama, Christophe Tribouilloy, Henry Sevestre, Sabrina Poirot, Philippe Giummelly, Jeffrey Atkinson, Gabriel Choukroun, Michel Andrejak, Said Kamel, Jean Claude Mazière and Ziad A. Massy

Circulation. 2009;119:306-313; originally published online December 31, 2008;
doi: 10.1161/CIRCULATIONAHA.108.797407
Circulation is published by the American Heart Association, 7272 Greenville Avenue, Dallas, TX 75231

Print ISSN: 0009-7322. Online ISSN: 1524-4539